


ARTICLE

Open Access



A novel 1,3,4-thiadiazole modified chitosan: synthesis, characterization, antimicrobial activity, and release study from film dressings

Ahmad E. Mohamed¹, Walid E. Elgammal¹, Aya M. Dawaba², Ahmed G. Ibrahim^{1*} , Amr Fouda³ and Saber M. Hassan¹

Abstract

Herein, two new polymers designated as Cs-EATT and Cs-BATT have been synthesized via linking the chitosan with the synthesized 1,3,4-thiadiazole compounds. They were characterized using ¹H, ¹³C-NMR, FT-IR, TGA, Elemental analysis, Mass spectrum, and UV–vis spectrophotometer. The synthesized polymers exhibit high activity to control the growth of pathogenic bacteria (*S. aureus*, *B. subtilis*, *E. coli*, and *P. aeruginosa*), and unicellular fungi (*C. albicans*). The MIC values were in the range of 25–100 μg mL⁻¹ for Cs-EATT and 25–200 μg mL⁻¹ for Cs-BATT with varied clear zones. The new polymers were mixed with three film-forming agents: polyvinyl alcohol, hydroxyethyl cellulose, and carboxymethyl cellulose to form six film dressings designated as E1, E2, and E3 for Cs-EATT, and B1, B2, and B3 for Cs-BATT, respectively. The evaluation of film dressings showed that the formed films had transparency, uniformity, homogeneity, elasticity, and non-irritation pH values for skin within the normal range. The maximum percentages of Cs-E/B-ATT content were recorded for film dressings E2 and B2, with values of 92.5% and 94.9%, respectively. Also, the release percentages varied according to film dressing formulation, with values in the ranges of 83.88–93.2% for Cs-EATT and (87.7–97.35%) for Cs-BATT after 9 h.

Keywords: Thiadiazoles, Chitosan, Antimicrobial activity, Pharmacological activity, Film dressings

Introduction

Biodegradable polymers have been of interest to many researchers for many years due to their ability to protect against many life-threatening diseases. Film dressings are considered an important segment of the medical and pharmaceutical markets worldwide. These compelling features make film dressings a versatile tool that has been exploited in drug delivery [1, 2].

Heterocyclic compounds are the most common and important scaffolds found in a wide range of bioactive natural products, synthetic drugs, pharmaceuticals, and

agrochemicals, and they are one of the most important classes of organic compounds used in a diversity of biological fields due to their activities in a variety of diseases. Among the numerous heterocycles, 1,3,4-Thiadiazole was first defined in 1882 by Fischer and further advanced by Busch and his co-workers [3]. Thiadiazoles are a heterocycle group with a five-membered ring that possesses sulfur and two nitrogen atoms and exhibit a broad range of biological activities [4, 5]. A significant number of molecules bearing the thiadiazole moiety have a variety of biological characteristics, such as antimicrobial [6, 7], antiproliferative [8], antitumor [9], antitubercular [10], anti-inflammatory [11], anticonvulsant [12], antioxidant [13], antileishmanial [14], antibacterial [15, 16], antiviral [17], analgesic [18], antipsychotic [19], antihistamine [20], anti-depressive [21], and antihypertensive [22].

*Correspondence: ahmed_polytech@azhar.edu.eg; ahmed_polytech@yahoo.com

¹ Department of Chemistry, Faculty of Science (Boys), Al-Azhar University, El-Nasr road, Nasr city, Cairo 11751, Egypt
Full list of author information is available at the end of the article

Chitosan is a biopolymer that is obtained from a large number of terrestrial and marine sources. It's considered a natural cationic polysaccharide because it's made up of deacetylated chitin, which is a hydrophilic linear polysaccharide made up of glucosamine and N-acetyl glucosamine units linked by β -(1-4) glycosidic bonds [23, 24]. It is widely used in the biomedical field due to its chemical, cosmetic, and pharmacological properties. Chitosan has many advantages, the most important of which are biocompatibility, biodegradability, and non-toxicity [25]. Moreover, several studies have indicated its bactericidal and fungicidal activities [26–29].

Topical delivery of the drug can improve its bioactivity due to its side effects, enhancing its penetration, ease of handling and administering, accurate dosage, and portability [30]. Polyvinyl Alcohol (PVA), Hydroxyethyl Cellulose (HEC), and Carboxymethyl Cellulose (CMC) were employed as the film forming agents, while PEG-400 was the plasticizer used. Topical film formulations for drug delivery have many advantages, the most important of which are their ability to spread easily, emollient effect, ease of removal, thixotropic properties, and the drug release through the skin to the tissue or precisely the target cell. The release of a drug from topical formulations depends on the physical and chemical nature of the components used and the activity of the drug [31, 32].

Therefore, the main hypothesis of the current study was to form two polymers via functionalization of chitosan with new heterocyclic compounds and evaluate their activity against pathogenic microbes and the possibility of incorporating them into film dressing formulations. The ^1H , ^{13}C -NMR, FT-IR, TGA-DTG-DSC, Elemental analysis, Mass spectrum analysis, and UV-vis spectrophotometer were used to characterize two synthesized polymers. The antimicrobial activity was assessed versus *Staphylococcus aureus* and *Bacillus subtilis* as Gram-positive bacteria, *Escherichia coli* and *Pseudomonas aeruginosa* as Gram-negative bacteria, and *Candida albicans* as a unicellular fungi. Moreover, three film-forming agents, polyvinyl alcohol (PVA), hydroxyethyl cellulose (HEC), and carboxymethyl cellulose (CMC) were used to form various film dressing formulations after adding polymers.

Experimental work

Materials

Chemicals and solvents such as chitosan (DD of 70–95%), thiosemicarbazide, (bromomethyl) benzene (PhCH_2Br), iodoethane ($\text{C}_2\text{H}_5\text{I}$), dichloromethane (DCM, HPLC), and ethanol (95% and 99%) were offered by Sigma-Aldrich. Carbon disulfide (CS_2), thionyl chloride (SOCl_2), toluene, hydrochloric acid, sodium carbonate, dimethyl sulfoxide (DMSO), and triethanolamine were bought from Alfa Aesar and El-Nasr companies, Egypt. The

following: Polyvinyl Alcohol (PVA), Hydroxyethyl Cellulose (HEC), and Carboxymethyl Cellulose (CMC) were purchased from CISME Italy SRL. The precursor of succinic anhydride was prepared according to the literature [33].

Methods

Synthesis procedure of 5-amino-1,3,4-thiadiazole-2-thiol [A-TT] [34, 35]

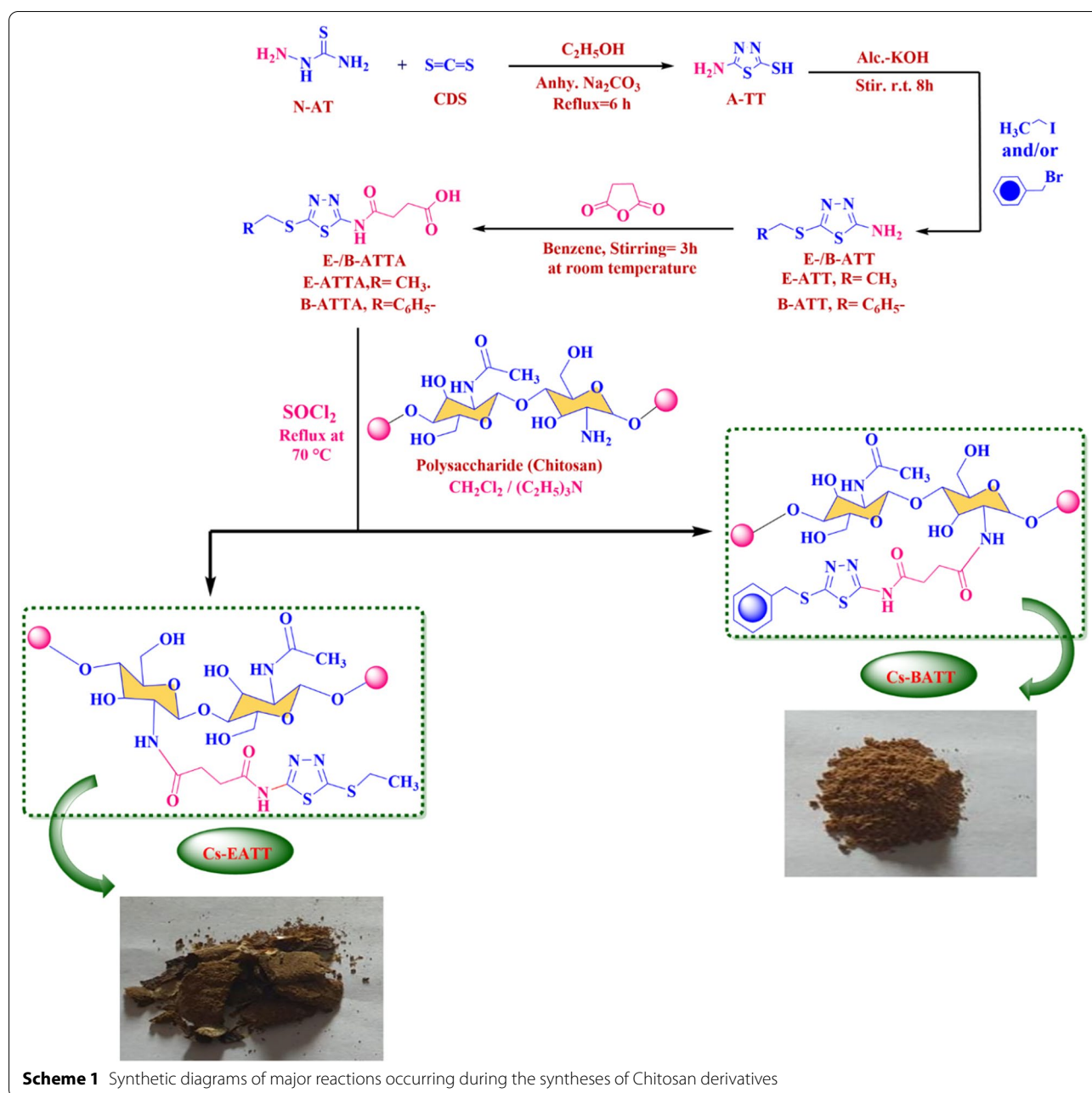
In this experiment, carbon disulfide (0.25 mol) was added dropwise to a stirred solution of N-amino-thiourea (0.25 mol) and sodium carbonate (0.23 mol) in ethanol (15 ml). The mixture was stirred under reflux for 1 h. After that, the mixture was heated at 75–80 °C in a water bath for 4 h. Ethanol was evaporated in the vacuum and the remaining solid was poured into ice-cold water and treated with concentrated HCl. The precipitated out was filtered, washed with cold water, and recrystallized from ethanol to give the compound as yellowish-white crystals. Yield: 78% (m.p: 238–239 °C).

General synthesis to get 5-(ethyl/benzylthio)-1,3,4-thiadiazol-2-amine [E-/B-ATT] [36, 37]

In a 100-ml Erlenmeyer conical flask equipped with a magnetic stirring bar, charged with a suspension of A-TT (0.1 mol, 13.3 g) in $\text{C}_2\text{H}_5\text{OH}$ (95%) (20 mL), 0.1 mol of potassium hydroxide was added in three portions and stirred at ambient temperature for 0.5 h. The reaction mixture was cooled to 0 °C in an ice bath, and alkylating agents, such as ethyl iodide and/or benzyl bromide (0.1 mol) were dropped during a period of fifteen minutes of vigorous stirring. After the addition is complete, the cooling bath is removed, and the mixture is allowed to come to room temperature. The reaction mixture was swirled for an additional period of 8 h at room temperature. The solid product was filtered, followed by washing with water and recrystallization from ethanol/water to furnish the desired product. The recovery of the solid product from the recrystallization solvent was performed by cooling in air, then filtration, followed by washing with ethanol.

General synthesis of 1,3,4-thiadiazol containing carboxylic acid fragments [E-/B-ATTA]

To a stirred solution of ethyl/benzyl thiadiazole derivatives (0.01 mol) in dry benzene (30 ml), dihydrofuran-2,5-dione (0.02 mol) was added in three portions. The solution was robustly stirred for 3 h at room temperature. At the end of this period, the crude solid was separated as pale yellow or white crystals, which were collected on a suction filter, washed with ethanol, and air-dried. Recrystallization was done from ethanol or an ethanol/benzene mixture to afford the final product, as highlighted



in Scheme 1, and the recovery of the product from the recrystallization solvent was performed by cooling in air, then filtration, followed by washing with ethanol.

General procedure for one-pot synthesis of chitosan derivatives [Cs-E/B-ATT]

To a rapidly stirred cooled mixture of thiazazole carboxylic acid derivatives (E/B-ATTA, 0.01 mol) and the polysaccharide (chitosan, 0.01 mol) in the presence of triethyl amine (Et_3N , 0.03 mol) in dichloromethane (DCM, 100 ml) in an ice bath, freshly distilled sulphurous

oxychloride (SOCl_2 , 0.13 mol) is added dropwise (3–5 drops/second) from the dropping funnel. When the addition is finished, the bath is removed, the mixture is stirred and heated to reflux at 70 °C overnight. The mixture is then cooled, filtered through an 8-in. Büchner funnel, and washed three times with DCM to give the new chitosan derivative, as shown in Scheme 1.

Instruments specifications

$^1\text{H-NMR}/^{13}\text{C-NMR}$ spectra were done using a solution of deuterated DMSO-d_6 on JNM-ECA 500 II Made by

JEOL-JAPAN instrument, at 500 and 125 MHz, respectively. Proton chemical shifts are reported in δ scale (ppm) downfield from TMS. The multiplicity utilized is as follows: [s: singlet, d: doublet, t: triplet, q: quartet, and m: multiple]. The residual protons (2.50 and 3.31 ppm) were used as the internal references. FT-IR was inscribed through the Nicolet iS10FT IR Spectrometer, Thermo Fisher Scientific Resolution 16 on (KBr disc) (n cm^{-1}) technique. Shimadzu Japan's GC-2010 was used for the GC-MS analysis. Fusion points were verified on the SMP50 Digital Melting Point APP (Bibby Scientific, Staffordshire, UK) 120/230 V instrument and were left uncorrected. Thermogravimetric analysis of the samples was performed using Discovery SDT 650-Simultaneous DSC-TGA/DTA Instruments, USA. The sample was heated under nitrogen from 0 to 500 °C (10 °C/min). The elemental analysis was carried out at the Microanalytical Center, Cairo University, Giza, Egypt using the Elemental C-H-N-S AnalyzerVario El M, Germany. All the data was within $\pm 0.4\%$ of the theoretical values. UV Spectrophotometer, model 6705, Jenway. pH metre AD-1030 pH mV & Thermometer, Adwa, Romania. MXBAOHENG Lab Digital Electric Mixer, Overhead Stirrer, Laboratory Mixer Agitator, Suma, UK. Hotplate Multi-position magnetic stirrer with heater SB 162-3, Stuart, UK.

Biological activities of chitosan derivatives

Antimicrobial activity

Antimicrobial activity of the stock solution The activity of two synthesized chitosan derivatives designated as Cs-EATT and Cs-BATT to control the growth of pathogenic Gram-positive bacteria (*Staphylococcus aureus* ATCC6538 and *Bacillus subtilis* ATCC6633), Gram-negative bacteria (*Escherichia coli* ATCC8739 and *Pseudomonas aeruginosa* ATCC9022), and *Candida albicans* ATCC10231 (unicellular fungi) was assessed by the agar well diffusion technique [38]. Each bacterial and fungal strain was refreshed by inoculating on an appropriate medium (nutrient broth for bacteria and yeast extract peptone dextrose (YEPD) broth for *Candida* sp.) overnight at 35 ± 2 °C. At the end of the incubation period, adjust the optical density (O.D.) for each strain to 1.0. Under aseptic conditions, approximately 50 μL from each strain was pipetted onto the center of the sterilized petri dish, poured cooled Muller Hinton agar media (for bacteria) and/or YEPD agar media (for *Candida* sp.), and mixed well. Upon media solidification, wells (0.6 cm in diameter) were made in each plate and filled with 100 μL of prepared solution ($300 \mu\text{g mL}^{-1}$) and transferred to the refrigerator for one hour before being incubated at 35 ± 2 °C for 24 h. The results were recorded as the diameter of the clear zone around each well (mm). The experiment was carried out in triplicate. As part of the experiment, dimethyl

sulfoxide (DMSO, solvent system) was used as a negative control, whereas penicillin G (for G+), Ciprofloxacin (for G-), and ketoconazole (for *Candida albicans*) were run as positive controls [39].

Determination of MIC value The highest concentration ($300 \mu\text{g mL}^{-1}$) of synthesized chitosan derivatives exhibited antimicrobial activity against all tested microbes. Therefore, various concentrations (200, 100, 50, 25, and $12.5 \mu\text{g mL}^{-1}$) were prepared from each synthesized derivative to detect the value of the minimum inhibitory concentration (MIC) using the agar well diffusion method. Approximately 50 μL from each bacterial and/or fungal strain was pipetted onto a sterilized petri dish, followed by pouring cooled Muller Hinton agar media (for bacteria) and/or YEPD (for *Candida albicans*) over the inoculum and mixing well. After that, 100 μL of each prepared concentration was added to wells (0.6 mm) prepared in the solidified plate before being kept in the refrigerator for one hour. The loaded plates are incubated for 24 h at 35 ± 2 °C. The MIC value was recorded as the lowest concentration that has the efficacy to inhibit microbial growth [40, 41].

Film dressing

Preparation of stock solutions and detecting their maximum absorbance (λ_{max}) The stock solution of Cs-E/B-ATT was prepared by dissolving 100 mg of chitosan derivative in 100 ml of phosphate buffer (pH = 6.8) containing 10% w/w of DMSO to improve the solubilization in a volumetric flask with continuous shaking. Here, DMSO was added to enhance the solubility adjuvant advantage as a penetration enhancer, which led to improved skin absorption of Cs-E/B-ATT [42]. To get $10 \mu\text{g mL}^{-1}$ of solution, 1 ml of stock solution was withdrawn and diluted to 100 ml of phosphate buffer (pH = 6.8) with 10% w/w of DMSO. After that, the maximum absorption (λ_{max}) of Cs-E/B-ATT solutions ($10 \mu\text{g mL}^{-1}$) was determined using a UV-Visible spectrophotometer at wavelengths of 200–400 nm.

Preparation of film dressings formulations of Cs-E/B-ATT

The main purpose of this preparation is to develop a more efficient Cs-E/B-ATT pharmaceutical application that can be used in a broad range of biomedical disciplines in the form of film dressings to benefit from its antimicrobial activity. A series of polyvinyl alcohol (PVA), hydroxyethyl cellulose (HEC), and carboxymethyl cellulose (CMC) were used as film-forming agents (FFA) for the formulation of proper film dressings of Cs-E/B-ATT. Six formulae were prepared and designated as follows: E1–E3 for Cs-EATT and B1–B3 for Cs-BATT using PVA, HEC, and CMC, respectively. Approximately 1 gm of FFA was dispersed in 20 ml of distilled water by using a magnetic stirrer at 50 °C.

After that, an adequate concentration (0.4 g/20 ml) of Cs-E/B-ATT was added to the previous mixture to prepare film dressings. Following that, 0.2 mL of the employed plasticizer, PEG-400, was added. The clear solution was poured into the Petri-dishes (have a diameter of 8 cm). To avoid film stickiness, the plate was lubricated with a swap of glycerin [42, 43].

Evaluation of Cs-E/B-ATT dressing films

Thickness and weight variation The thickness of the formulated Cs-E/B-ATT dressing films was detected using a Vernier caliper. The measurement was achieved in triplicate at different points on the film. Whereas the weight of formulated dressing films was determined by digital balance. Three uniform pieces ($1 \times 1 \text{ cm}^2$) at random places on each film were weighed to determine the weight variation, and the average weight was calculated [44].

Folding endurance Folding endurance of the Cs-E/B-ATT dressing films was determined manually by using forceps. Folding the Cs-E/B-ATT film in the center and then opening it was considered one folding. The number of counts, folding the inserts at the same place without breaking, was reported as the value of folding endurance [45].

Tensile strength The tensile strength of the Cs-E/B-ATT dressing films was evaluated using Brookfield CT3 texture analyzer equipment (Middleboro, MA, USA). Films are held between two clamps positioned at a distance of 3 cm. During measurement, the films were pulled at a rate of 50 mm/min. The results were taken in triplicate. The tensile strength was calculated according to the following equation [46].

$$TS = \frac{L}{T} \times W_d \quad (1)$$

where TS is the tensile strength, L is a load at breakage, T is the strip thickness, and W_d is the strip width.

% Moisture absorption This test is important to check the stability of the film formulations. The initial weighting of each formula was performed, and then they were kept in aluminum chloride desiccator to attain 79.5% moisture, then after 3 days, the formulations were taken out and assessed by weight according to the following equation [47].

$$M_a = \frac{W_f - W_i}{W_i} \times 100 \quad (2)$$

where M_a is the percentage of moisture absorption, W_i is the initial weight of the film, and W_f is the final weight of the film.

% Moisture loss This experiment is important to check the drying of the film formulations. The initial weighting of each formula was performed, and then they were kept in anhydrous calcium chloride desiccator, then after 3 days, the formulations were taken out and assessed by weight according to the following equation [47].

$$M_L = \frac{W_i - W_f}{W_i} \times 100 \quad (3)$$

where M_L is the percentage of Moisture loss, W_i is the initial weight of the film, and W_f is the final weight of the film.

Determination of surface pH The pH of the Cs-E/B-ATT film was monitored using a pH meter that had been calibrated with a standard buffer solution before each use. The measurements were taken in triplicate at ambient temperature.

Content of Cs-E/B-ATT In a volumetric flask, 0.1 gm of each produced film was dissolved in 15 ml of phosphate buffer (pH = 6.8) with 10% (w/w) DMSO and well shaken to achieve total solubility, and then the solution was filtered through Millipore filter paper (0.45 μm). A UV-Spectrophotometer was used to determine the absorbance of the solution at 285 nm for Cs-EATT and 280 nm for Cs-BATT [48].

In-vitro Cs-E/B-ATT release studies

This experiment was performed using Spectra Pore dialysis membrane tubing as follows: in a cellulose membrane tubing (with a molecular weight cut-off of 12,000–14,000), 0.1 g of each prepared film was loaded, then both ends of the tube were closed well. After that, the tubes were soaked overnight in the dissolution tester, which contains 50 ml of phosphate buffer (pH = 6.8) with 10% (w/w) DMSO at a temperature of $37 \pm 0.5 \text{ }^\circ\text{C}$. At predetermined intervals, a certain amount from each sample was taken and replaced with an equal amount of new phosphate buffer to maintain the sink condition. The taken samples were filtered with a membrane filter (0.45 μm) (Double Ring Filter Paper 12.5 cm chart) and assayed by using UV-Vis at λ_{max} 285 and 280 nm for Cs-EATT and Cs-BATT, respectively. The concentration of the Cs-E/B-ATT samples was determined by applying the linear equation obtained by plotting a calibration curve over the concentration range (1–10 $\mu\text{g ml}^{-1}$). Each experiment was performed three times, and the *in-vitro* release studies were carried out over a 12 h period [49].

Kinetic analysis

In-vitro release data were analyzed using mathematical kinetic equations (Table 1) based on zero-order, first-order, and diffusion kinetic models (Higuchi model).

Statistical analysis

The obtained data in the current study were subjected to analysis of variance (ANOVA) by using SPSS v17 (IBM, Armonk, NY, USA). The significant difference between various treatments was analyzed by the Tukey HSD test at $p < 0.05$.

Results and discussion

FT-IR analysis

E-ATTA (Additional file 1: Fig. S1a): 3363 cm^{-1} (O–H stretching), 3148 cm^{-1} (N–H stretching vibrations), 2927 cm^{-1} (C–H stretching vibrations (aliphatic)), 1708 cm^{-1} (C=O stretching vibrations (acid)), 1686 cm^{-1} (C=O stretching (amide)), 1560 cm^{-1} (C=N stretching vibrations), 1452 cm^{-1} (HC=CH stretching vibrations), 1309 cm^{-1} (C–O stretching vibrations), 1088 cm^{-1} (S–C–S stretching vibrations). Cs (Additional file 1: Fig. S1b): 3400–3460 cm^{-1} (O–H & N–H stretching (amide II)), and intra-molecular hydrogen bond of –OH...O on saccharine ring), 2929 cm^{-1} and 2880 cm^{-1} (C–H, asym. and sym. stretching vibrations), 1659 cm^{-1} (C=O stretching vibration (amide I) and C=O...H–N hydrogen bond), 1596 cm^{-1} (N–H bending vibration (amide II)), 1430 cm^{-1} (–CH₂– bending and rocking vibrations), 1380 cm^{-1} (–CH– asymmetric bending vibration), 1080 cm^{-1} and 1030 cm^{-1} (C–O stretching vibrations), and 895 cm^{-1} (stretching vibration of saccharine ring) [53, 54]. Cs-EATT (Additional file 1: Fig. S1c): 3441 cm^{-1} (O–H and N–H stretching vibration), 2924 cm^{-1} (C–H stretching vibration (aliphatic)), 1726 cm^{-1} (C=O stretching vibration (amide)), 1714 cm^{-1} (C=O stretching vibration (amide)), 1632 cm^{-1} (C=N stretching vibration), 1555 cm^{-1} (HC=CH stretching vibration), 1083 cm^{-1} (S–C–S stretching vibration), 1125 cm^{-1} (C–O–C asymmetric stretching vibration of glucosamine), and 1064 and 1023 cm^{-1} (C–O stretching vibration of glucosamine).

B-ATTA (Additional file 1: Fig. S2a): 3605 cm^{-1} (O–H stretching), 3201 cm^{-1} (N–H stretching), 3059 cm^{-1} (C–H stretching (aromatic)), 2971 cm^{-1} (C–H stretching (aliphatic)), 1693 cm^{-1} (C=O stretching (acid)), 1678 cm^{-1} (C=O stretching (amide)), 1572 cm^{-1} (C=N stretching), 1553 cm^{-1} (C=C stretching), 1300 cm^{-1} (C–O stretching), 1053 cm^{-1} (S–C–S stretching). Cs-EATT (Additional file 1: Fig. S2c): 3415 cm^{-1} (O–H and N–H stretching vibration), 3001 cm^{-1} (C–H stretching vibration (aromatic)), 2928 cm^{-1} (C–H stretching vibration (aliphatic)), 1796 cm^{-1} (C=O stretching vibration (amide)), 1733 cm^{-1} (C=O stretching vibration (amide)), 1632 cm^{-1} (C=N stretching vibration), 1538 cm^{-1} (C=C stretching vibration), 1133 cm^{-1} (C–O–C asymmetric stretching vibration of glucosamine), 1070 cm^{-1} (S–C–S stretching vibration), and 1053 and 1011 cm^{-1} (C–O stretching vibration of glucosamine).

¹H & ¹³C NMR and mass analysis

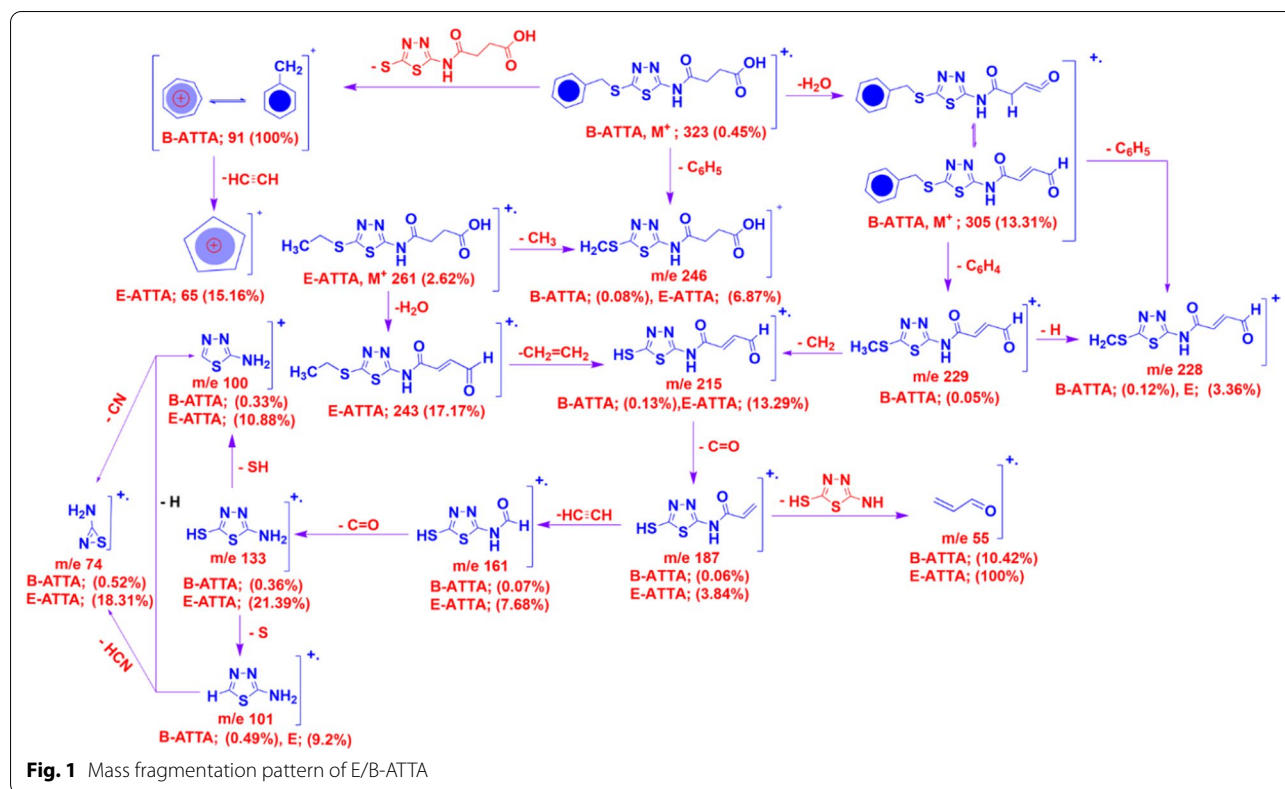
E-ATTA (Additional file 1: Fig. S3a,b): 12.61 (s, 1H, O–H, exchangeable by D₂O), 12.23 (s, 1H, NH, exchangeable by D₂O), 3.17 (q, 2H, CH₃CH₂–S–), 2.66 (t, 2H, CH₂–COOH), 2.53 (t, 2H, CH₂–CONH–) and 1.3 (t, 3H, CH₃CH₂–S–). ¹³C-NMR (Additional file 1: Fig. S3c): 173.56 (C=O (acid)), 170.80 (C=O (amide)), 158.61 (–S–C–S), 158.45 (–S–C–NH), 29.89 (–CH₂–COOH), 28.37 (CH₃CH₂–S–), 28.15 (–CH₂–CONH–) and 14.80 (CH₃CH₂–S–). The molecular formula of E-ATTA was further confirmed by mass spectrometry analysis (Fig. 1) showing the peak at m/z 261 (2.62%) corresponding to the molecular ion, which losses H₂O, CH₂=CH₂, CO, HC≡CH, CO, S, and HCN successively to produce ion fragment peaks at 243.01 (17.17%), 215 (13.29%), 187 (3.84%), 161 (7.68%), 133 (21.39%), 101 (9.2%), and 74 (18.31%), respectively as shown in Fig. 1, and the base peak was observed at 55 (100%) correspond to vinyl carbonyl (C₃H₃O⁺) fragment ion.

B-ATTA (Additional file 1: Fig. S4a): 12.62 (s, 1H, O–H), 12.23 (s, 1H, NH), 7.39–7.24 (m, 5H, Ar–H), 4.46 (s, 2H, Ph–CH₂–S–), 2.67 (t, 2H, CH₂–COOH) and 2.54 (t, 2H, CH₂–CONH–). ¹³C-NMR (Additional file 1: Fig. S4b): 173.51 (C=O (acid)), 170.81 (C=O (amide)), 158.92 (–S–C–S), 157.88 (–S–C–NH), 136.77, 129.01, 129.01, 128.61, 128.61, 127.63 (aromatic carbons), 37.61 (CH₂–S–), 29.83 (–CH₂–COOH) and 28.30 (–CH₂–CONH–). Further, the resulting compound was confirmed by mass spectrum (Fig. 1) which showed the molecular ion peak at m/z = 323 (0.45%) which losses H₂O, C₆H₄, CH₂, CO, HC≡CH, CO, S, and HCN successively to produce ion fragment peaks at 305 (13.3%), 229 (0.05%), 215 (0.13%), 187 (0.06%), 161 (0.07%), 133 (0.30%), 101 (0.49%), and 74 (0.52%),

Table 1 Mathematical kinetic equations used in this study

Kinetic model	Mathematical equation	Eq. no.	References
Zero-order model	$A_t = A_0 + K_0 t$	(4)	[50]
First-order model	$\log A_t = \log A_0 - (K_1/2.303)t$	(5)	[51]
Higuchi model	$A_t = K_H \times t^{0.5}$	(6)	[52]

Where A_t is the amount of drug released or dissolved at time t , A_0 is the initial amount of drug in the solution, K_0 is the zero-order release constant expressed in units of concentration/time, K_1 is the first-order rate constant, and K_H is the release rate constant for the Higuchi model



respectively, and the base peak observed at $m/z=91$ (100%) which attributed to tropylium ion.

Cs-EATT and Cs-BATT (Fig. 2a, b): configuration of Cs-EATT was as well, confirmed by the Nuclear magnetic resonance technique. $^1\text{H-NMR}$ of chitosan [55] elucidated the signals at (δ ppm): 1.32 ppm integrating for three protons of the methyl of the N-acetyl group in the Cs. In addition, the signals of H2-H2' in the glucosamine unit are at 2.80 ppm and 3.36 ppm (3.28–3.40 ppm). The numerous signals in the 3.6–4.15 ppm range due to the hydrogens of H3-H6 and the signals at 4.76, 5.11 ppm ascribe to the hydrogens of H1-H1' in the glucosamine moiety. As in Fig. 2a, the new signals at 1.17 ppm, 2.55 ppm, 2.68 ppm, 3.21 ppm, 9.83 ppm, and 12.64 ppm which were attributed to the resonance of the three protons of ($\text{CH}_3\text{CH}_2\text{-S}$), two protons of ($\text{CH}_2\text{-CONH-}$), two protons of ($\text{CH}_2\text{-COOH}$), two protons of ($\text{CH}_3\text{CH}_2\text{-S-}$) and two protons of (2NH) respectively, confirmed the formation of Cs-EATT. Also, NMR- d_6 of Cs-BATT (Fig. 2b), the absence of the singlet signal corresponding to O-H proton of acid, and the appearance of a new N-H signal at δ 9.17 ppm indicate the formation of the modified chitosan, with other requisite numbers of protons in its $^1\text{H-NMR}$ spectrum, supported the formation of the assigned structure as shown in Fig. 2b.

Elemental analysis

The elemental analysis results for Cs-EATT and Cs-BATT were presented in Table 2 and used to determine the degree of substitution (DS) according to Eq. 7 [55].

$$DS(\%) = \frac{x(C/N)_a - (C/N)_b}{y} \times 100 \quad (7)$$

where $(C/N)_b$ is the carbon/nitrogen ratio of Cs-EATT and Cs-BATT, $(C/N)_a$ is the carbon/nitrogen ratio of the chitosan. x and y are the numbers of nitrogen and carbon atoms, respectively, introduced into chitosan after modification with E-ATTA and B-ATTA compounds. The degree of substitution (DS) value was observed to be 84.7% for Cs-EATT and 44.1% for Cs-BATT.

TGA

The TGA was conducted to investigate the thermal behavior of the two functionalized chitosan, Cs-EATT and Cs-BATT, and the data obtained were tabulated in Table 3 on the basis of the plot of mass loss (%) versus temperature, as presented in Fig. 3. From the figure, both samples undergo a decrease in mass as the temperature increases. Meaning that the stability of both samples is temperature-dependent. Comparing the data presented in Table 3 indicates that the thermal stability

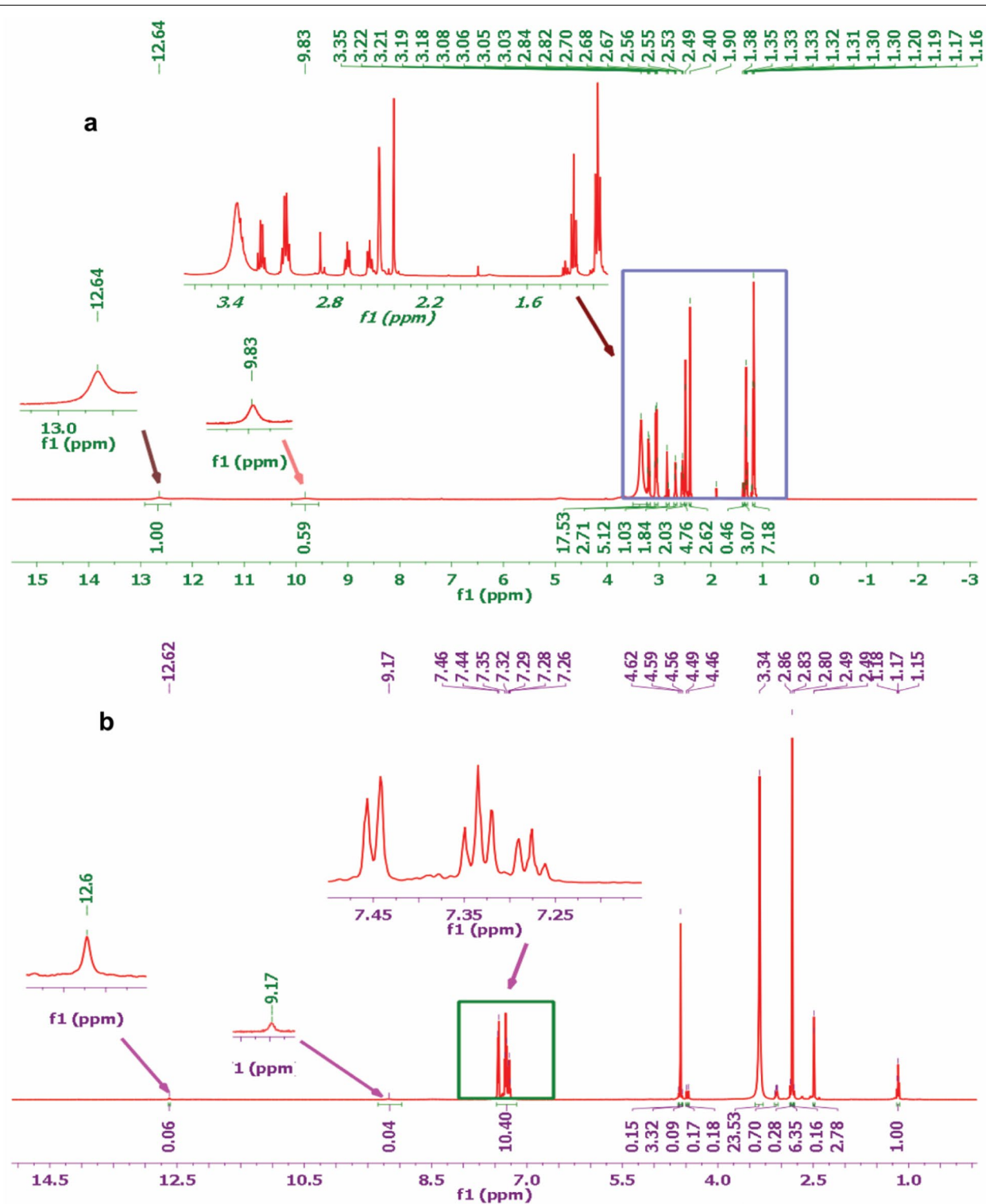


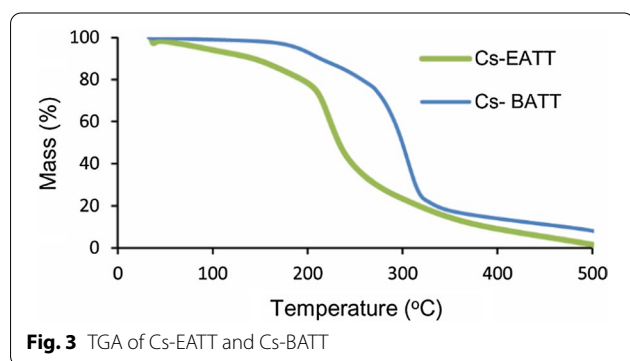
Fig. 2 **a** ¹H-NMR of Cs-EATT and **b** ¹H-NMR of Cs-BATT

Table 2 Elemental analysis and degree of substitution of Cs-EATT and Cs-BATT

Compound	Element (%)				x	y	C/N	DS (%)
	C	H	N	S				
Cs-EATT	36.21	5.63	8.90	7.06	3	8	4.07	84.7
Cs-BATT	47.57	4.54	12.79	10.51	3	13	3.72	44.1

Table 3 Mass loss data obtained from TGA analysis for Cs-EATT and Cs-BATT

Functionalized chitosan	Mass loss (%) at temperature (°C)					T ₅₀ (°C)
	100	200	300	400	500	
Cs-EATT	5.94	21.63	76.56	90.92	98.38	232.97
Cs-BATT	1.00	6.99	50.40	85.97	91.84	299.73



of Cs-BATT is higher than that of Cs-EATT. This may be due to the presence of phenyl groups in Cs-BATT which restrict the mobility of the chains, hence the stability increases. The initial loss in the sample mass with temperature corresponds to the desorption of the moisture. The mass loss propagation is due to the decomposition of the heterocyclic moieties followed by the decomposition of the D-glucosamine rings. As shown in Table 3, the T₅₀ (The temperature at which the sample losses half of its mass) of Cs-EATT is lower than that of Cs-BATT by 67 °C. This confirms the result that the thermal stability of Cs-BATT is higher than that of Cs-EATT.

Antimicrobial activity

Recently, studies of functionalized chitosan with new active compounds have increased to provide a wide range of biomedical and biotechnological chitosan applications [35, 56, 57]. The chemical modifications of chitosan to form new functional characteristics are important steps to overcome the low solubility of chitosan that hinders its applications [58]. The solubility of chitosan was increased in the presence of hydrophilic thiazole derivatives, as reported previously [59]. Therefore, the antibacterial

and antifungal activities of newly synthesized functionalized chitosan with ethyl and benzyl thiazole, Cs-EATT, and Cs-BATT were evaluated against *Bacillus subtilis*, *Staphylococcus aureus*, *Escherichia coli*, *Pseudomonas aeruginosa*, and *Candida albicans* by the agar well diffusion method. The DMSO (solvent system) did not exhibit any antimicrobial activity against any of the tested bacterial or fungal strains. For *B. subtilis*, the differences between the zone of inhibition formed due to treatment with 300 µg mL⁻¹ are non-significant between Cs-EATT (19.8 ± 0.3 mm) and Penicillin (19.7 ± 0.6 mm), while it was highly significant ($p \leq 0.001$) as compared with the zone formed due to Cs-BATT (14.7 ± 0.7 mm) (Fig. 4a). In contrast, the zones of inhibition formed due to the treatment of *S. aureus*, *P. aeruginosa*, and *C. albicans* with the highest concentration (300 µg mL⁻¹) of functionalized Cs-EATT and Cs-BATT represent a significant difference. Data analysis showed that the activity of Cs-EATT was higher than that of Cs-BATT against all tested organisms except *C. albicans* (Fig. 4e). This phenomenon can be attributed to the presence of thiazole attached to the benzyl moiety. The current study is in harmony with those recorded by Li and co-author [59], who showed that the highest activity of functionalized chitosan with thiazole, methyl thiazole, and phenyl thiazole against three phytopathogenic fungi was achieved at a concentration of 1000 µg mL⁻¹. The authors attributed the activity of functionalized chitosan against phytopathogens to the presence of different thiazole derivatives.

To integrate the synthesized chitosan derivatives into various biomedical applications, they should be able to detect the lowest concentration that inhibits the growth of pathogenic microbes, which is known as a minimum inhibitory concentration (MIC). Therefore, the efficacy of different concentrations (200, 100, 50, 25, and

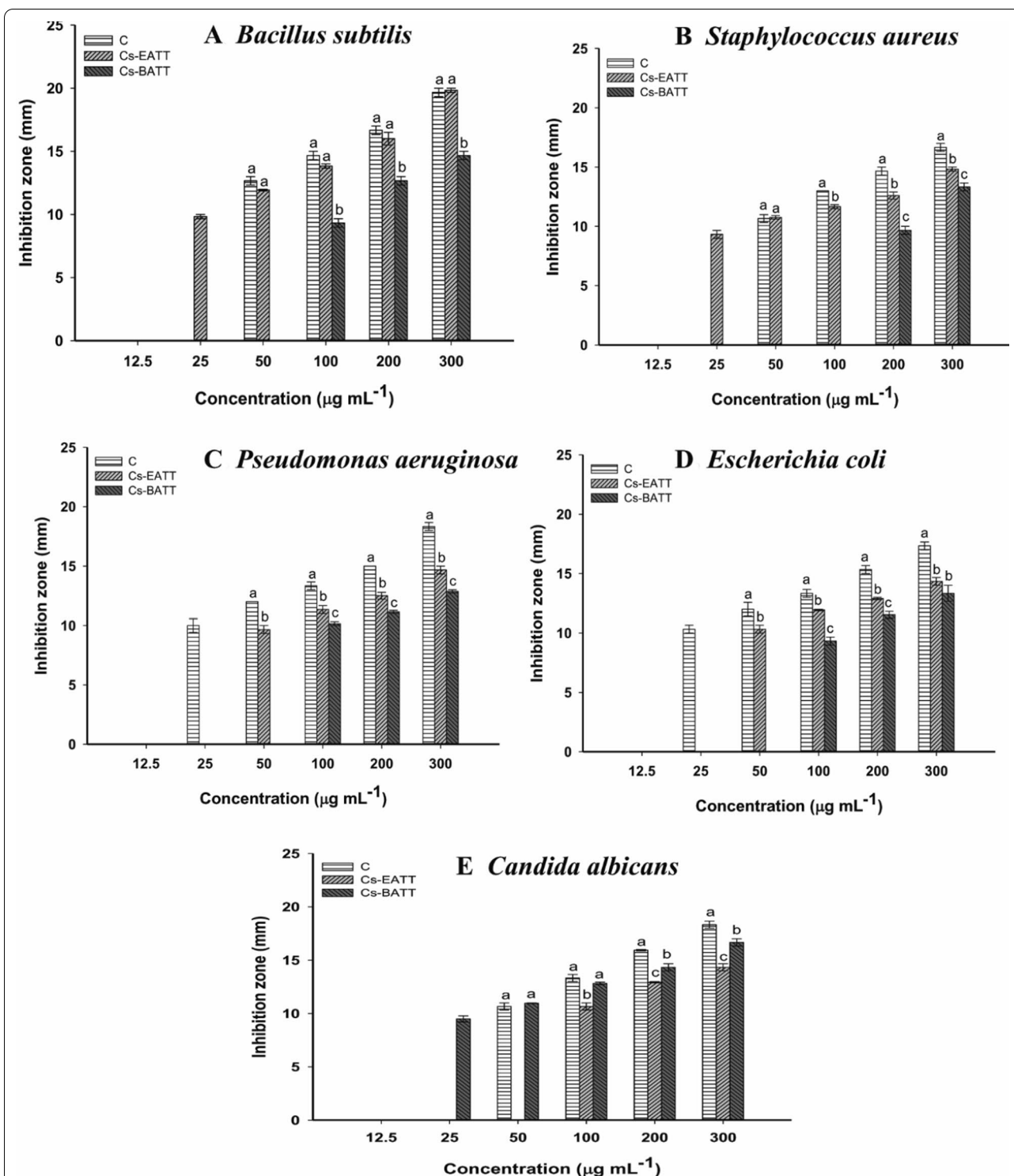


Fig. 4 Antimicrobial Activity of Cs-EATT and Cs-BATT compared with positive control against Gram-positive [*B. subtilis* (A), *S. aureus* (B)], Gram-negative bacteria [*P. aeruginosa* (C), *E. coli* (D)], and unicellular fungi [*C. albicans* (E)]

12.5 $\mu\text{g mL}^{-1}$) of two synthesized polymers, Cs-EATT and Cs-BATT, to control the growth of pathogenic Gram-positive bacteria, Gram-negative bacteria, and *C. albicans* was investigated. Data analysis showed that the activity of synthesized polymers is dependent on the concentration used. The activity decreases as the concentration is decreased. At 200 $\mu\text{g mL}^{-1}$, the zone of inhibition was decreased to (16.6 \pm 0.6, 13.0 \pm 0.0, 15.0 \pm 0.0, 15.3 \pm 0.6, and 15.9 \pm 0.1 mm), (16.0 \pm 0.9, 12.6 \pm 0.3, 12.5 \pm 0.5, 12.9 \pm 0.2, and 12.9 \pm 0.1), and (12.7 \pm 0.6, 9.7 \pm 0.1, 11.1 \pm 0.2, 11.5 \pm 0.5, and 14.3 \pm 0.6 mm) for positive control, Cs-EATT, and Cs-BATT against *B. subtilis*, *S. aureus*, *P. aeruginosa*, *E. coli*, and *C. albicans*, respectively. For Gram-positive bacteria, Cs-EATT was more active at low concentration as compared with positive control and Cs-BATT (Fig. 4a and b), whereas the functionalized chitosan with benzyl thiadiazole (Cs-BATT) was more active against *C. albicans* at low concentration as compared with control and Cs-EATT (Fig. 4e). The MIC values for positive control against *B. subtilis*, *S. aureus*, *P. aeruginosa*, *E. coli*, and *C. albicans* were 50, 50, 25, 25, and 50 $\mu\text{g mL}^{-1}$, respectively, whereas they were 25, 25, 50, 50, and 100 $\mu\text{g mL}^{-1}$ for Cs-EATT and 100, 200, 100, 100, and 25 $\mu\text{g mL}^{-1}$ for Cs-BATT with varied clear zones (Fig. 4a–e).

In our recent study, the functionalized chitosan with aminothiazole and imidazole carboxamide groups showed antimicrobial activity against Gram-positive bacteria (*B. subtilis* and *S. aureus*), Gram-negative bacteria (*P. aeruginosa* and *E. coli*), and *C. albicans* with MIC values ranging between 50 and 100 $\mu\text{g mL}^{-1}$ [57]. The antimicrobial activity of functionalized chitosan with active moieties was higher than that recorded by non-functionalized chitosan, as reported previously. For instance, chitosan loaded with ZnO nanoparticles showed stronger antimicrobial activity against *E. coli* and *S. aureus* than the activities recorded by chitosan without modification [60]. Moreover, the activity of composite magnetite/guar gum/chitosan to inhibit the growth of Gram-positive and Gram-negative bacteria was higher than that recorded by non-magnetite ones [61].

As reported previously [62], chitosan is characterized by its broad-spectrum activity against different pathogenic microbes, and their activity is increased by grafting with thiadiazole and other active moieties. The inhibitory effect of functionalized chitosan can be attributed to the various hypothesis, one of these hypotheses is related to cationic nature. The chitosan with a low molecular weight can easily penetrate the microbial cell walls and hence react with DNA and ultimately block the transcription process [63]. Whereas chitosan with a high molecular weight has the efficacy to bind with cell wall components with a negative charge and form an impermeable layer

surrounding the cell, which leads to a change in selective permeability function [64]. The grafting of chitosan with hydrophilic thiadiazole increases the solubility of chitosan and hence increases the electrostatic attraction between functionalized chitosan and the bacterial cell wall, which enhances cell mortality [65]. Another important inhibitory mechanism can be due to the production of reactive oxygen species as a result of accumulating the functionalized chitosan into the microbial cells and hence increasing cell mortality [66, 67]. Due to the disruption of the sterol profile existing in *C. albicans* cell wall because of negative impacts of treatment on the ergosterol synthesis pathway is considered another inhibitory mechanism of unicellular fungi [68].

Antimicrobial activity comparison study

Various attempts have been accomplished to investigate the antimicrobial activity of chitosan after modification or functionalization with various derivatives. Among these derivatives, are hydrophilic and hydrophobic thiadiazole (Table 4). For instance, chitosan was modified with different thiadiazole derivatives, including 1,3,4-thiadiazole; 2-methyl-1,3,4-thiadiazole, and 2-phenyl-1,3,4-thiadiazole and exhibited high growth inhibition percentages of different phytopathogenic fungi [59]. The highest growth inhibitions were achieved for modified chitosan with 2-methyl-1,3,4-thiadiazole with percentages of 75.3, 82.5, and 65.8%, respectively, against *Colletotrichum lagenarium*, *Phomopsis asparagi*, and *Monilinia fructicola*. Moreover, the antimicrobial activity of modified chitosan with 5-amino-1,3,4-thiadiazole-2-thiol; 5-phenyl-1,3,4-oxadiazole-2-thiol; and 5-(4-chlorophenyl)-1,3,4-thiadiazole-2-thiol against Gram-positive bacteria, Gram-negative bacteria, unicellular fungi, and multicellular fungi was higher than virgin chitosan [69]. In the current study, a new functionalized chitosan polymer with ethyl/benzyl thiadiazole derivatives showed high antibacterial activity against *S. aureus*, *B. subtilis*, *E. coli*, and *P. aeruginosa* as well as anti-*Candida* activity. Interestingly, there is no significant difference between the activity of modified chitosan and the positive control, which indicates the promising activity of modified chitosan to control the growth of pathogenic microbes.

Film dressing

Detection of λ_{max} for Cs-E/BATT

The wavelength of the prepared Cs-E/B-ATT was scanned at a range of 200–400 nm. The obtained data showed that the maximum absorbance of prepared Cs-EATT and Cs-BATT was observed at λ_{max} of 285 nm and 280 nm respectively.

Evaluation the quality of the prepared film dressing

The main criteria that confirm the successful formation of films are transparency, uniformity, homogeneity, elasticity, and texture properties [72]. At least one of these criteria is accomplished, as shown in Table 5.

Moreover, the thickness of the prepared film dressing was varied based on the modifications and film composition. As shown in Table 6, the thickness was varied in the ranges of 0.092 ± 0.01 – 1.12 ± 0.07 mm and 0.094 ± 0.01 – 1.06 ± 0.04 mm for Cs-EATT and Cs-BATT, respectively,

according to the film forming agent used. The change in thickness of the prepared film dressing followed the order of PVA > CMC > HEC and this phenomenon is compatible with the published study [47]. The weights of prepared film dressing were in the range of 4.5 ± 0.9 – 10.6 ± 1.2 mg and 4.3 ± 0.8 – 10.4 ± 1.3 mg for Cs-EATT and CS-BATT, respectively (Table 6). As shown, the highest weight was recorded for formulations of E1 and B1. The uniform distribution of the drug polymers and plasticizers is indicated by the weight uniformity of different films of the

Table 4 Comparing antimicrobial activity of various modified chitosan derivatives with those in the current study

New chitosan derivatives	Characterized by	Biological activities	Reference
Functionalized chitosan with 1,3,4-thiadiazole/2-methyl-1,3,4-thiadiazole/ and 2-phenyl-1,3,4-thiadiazole	FT-IR, ^{13}C NMR, and elemental analyses	Antifungal activity against three phytopathogenic fungi including <i>Colletotrichum lagenarium</i> , <i>Phomopsis asparagi</i> , and <i>Monilinia fructicola</i>	[59]
5-phenyl-1,3,4-oxadiazole-2-thiol/chitosan derivatives	FT-IR, TGA, and XRD	Antifungal activity against <i>Alternaria alternate</i> and <i>Fusarium</i> sp.	[70]
thiosemicarbazide-chitosan derivative	FT-IR, ^1H NMR, elemental analysis, XRD, and differential scanning calorimetric (DSC)	Antibacterial activity against <i>Escherichia coli</i>	[71]
Functionalized chitosan with 5-amino-1,3,4-thiadiazole-2-thiol; 5-phenyl-1,3,4-oxadiazole-2-thiol; 5-(4 chlorophenyl)-1,3,4-thiadiazole-2-thiol	FT-IR and ^1H NMR	- Antibacterial activity against <i>Escherichia coli</i> , <i>Aeromonas hydrophila</i> , <i>Shigella</i> sp., <i>Staphylococcus aureus</i> , <i>Bacillus subtilis</i> - Antifungal activity against <i>Candida albicans</i> and <i>Aspergillus niger</i>	[69]
Functionalized chitosan with ethyl/benzyl thiadiazole derivatives	^1H NMR, ^{13}C -NMR, FT-IR, TGA, Elemental analysis, Mass spectrum, and UV–vis spectroscopy	- Antibacterial activity against <i>Staphylococcus aureus</i> , <i>Bacillus subtilis</i> , <i>Escherichia coli</i> , and <i>Pseudomonas aeruginosa</i> - Antifungal activity against <i>Candida albicans</i>	Current study

Table 5 The physical characters of the prepared films

Items ^a	E1	E2	E3	B1	B2	B3
Transparent	✓	✓		✓	✓	
Stickiness		✓			✓	
Uniformity	✓		✓	✓		✓
Brittleness		✓			✓	
Elasticity		✓			✓	

^a The ✓ sign indicates the presence of the character checked

Table 6 The Evaluation parameters of different film dressing formulations

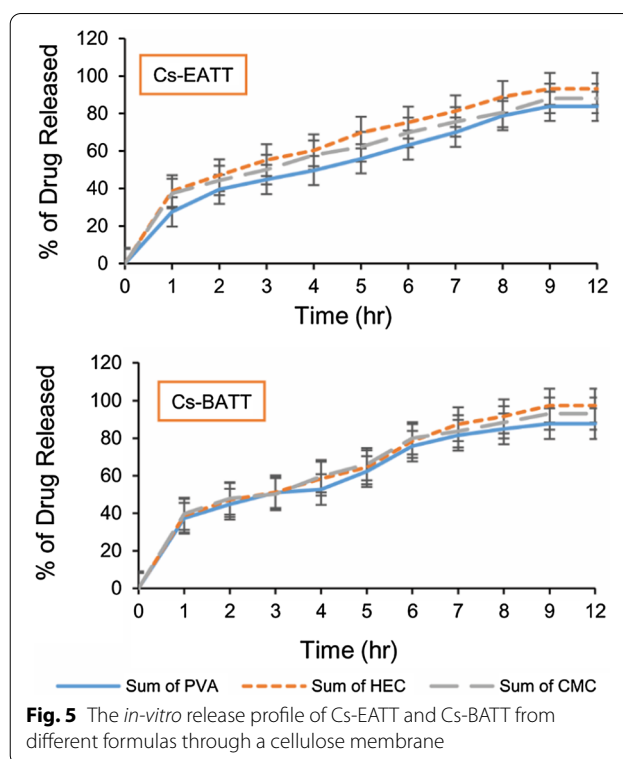
Film dressing formula	Thickness (mm)	Weight (mg)	Folding endurance	Tensile strength (Kg/mm ²)	Moisture Loss (%)	Moisture Absorption (%)	Surface pH	Drug Content (%)
E1	1.12 ± 0.07	10.6 ± 1.2	84 ± 2	5.72 ± 1.02	7.7 ± 0.3	12.3 ± 0.4	6.8 ± 0	85.9 ± 16.1
E2	0.063 ± 0.04	4.5 ± 0.9	24 ± 1	3.05 ± 0.09	11.2 ± 0.9	17.3 ± 0.3	6.3 ± 0.2	92.5 ± 26.5
E3	0.092 ± 0.01	7.4 ± 1.5	53 ± 3	1.06 ± 0.05	12.6 ± 0.5	22.6 ± 1.2	6.6 ± 0.1	88.2 ± 22.8
B1	1.06 ± 0.04	10.4 ± 1.3	93 ± 3	5.34 ± 1.03	6.8 ± 0.6	14.7 ± 0.7	6.9 ± 0.2	86.7 ± 16.5
B2	0.057 ± 0.01	4.3 ± 0.8	30 ± 1	2.96 ± 0.09	9.5 ± 0.7	15.4 ± 0.7	6.1 ± 0	94.9 ± 27.4
B3	0.094 ± 0.01	7.3 ± 1.7	62 ± 2	1.03 ± 0.07	14.3 ± 0.7	20.9 ± 2.02	6.5 ± 0.1	90.6 ± 18.8

same batch. The folding endurance was correlated with the film weight. This means the folding endurance was increased by increasing the film weight. The maximum folding endurance was recorded for the formulations of E1 (84 ± 2) and B1 (93 ± 3) and this is due to their highest weights (Table 6). Tensile strength is used to investigate the mechanical properties of the prepared film dressing. Data showed that the highest tensile strength was recorded for the formulations of E1 and B1 due to the presence of polyvinyl alcohol as a film-forming agent. The obtained data are compatible with those recorded by Asrofi and co-authors, who reported that the tensile strength of film-forming using PVA as the film-forming agent was higher than those formed using bengkuang starch and this attributed to the high crystallinity of PVA [73]. The PVA tends to form an intramolecular network between its chains, hence producing good mechanical characteristics [74].

The moisture percentage loss was in the range of 7.7 ± 0.3 , 11.2 ± 0.9 , and $12.6 \pm 0.5\%$ for formulations E1, E2, and E3, respectively, whereas it was 6.8 ± 0.6 , 9.5 ± 0.7 , and $14.3 \pm 0.7\%$ for formulations B1, B2, and B3, respectively. The decrease in moisture percentage loss was noted to follow the order of $\text{CMC} > \text{HEC} > \text{PVA}$ formulations due to hydrophobic characteristics. On the other hand, the moisture percentage absorption was highly varied between formulations and was (12.3 ± 0.4 , 17.3 ± 0.3 , and $22.6 \pm 1.2\%$) and (14.7 ± 0.7 , 15.4 ± 0.7 , and $20.9 \pm 2.02\%$) for (E1, E2, and E3) and (B1, B2, and B3), respectively (Table 6). The moisture absorption of the films followed the order $\text{CMC} > \text{HEC} > \text{PVA}$ formulations, and this is correlated with the hydrophilicity of the film forming agents. The main advantage of the different film dressings prepared in the current study was that their pH values were satisfactory (6.1–6.9) (Table 6), thereby avoiding the risk of skin irritation upon their applications. The drug content in each prepared film was assessed as shown in Table 6. The highest drug content was recorded for formulations E2 and B2 with percentages of $92.5 \pm 26.5\%$ and $94.9 \pm 27.4\%$ respectively, whereas the lowest drug content was recorded for formulations E1 ($85.9 \pm 16.1\%$) and B1 ($86.7 \pm 16.5\%$). These variations can be attributed to the film-forming agent used [72].

In-vitro drug release studies

The *in-vitro* release of Cs-E/B-ATT for the different formulas of (E1, E2, and E3) and (B1, B2, and B3) films was investigated using the dialysis membrane as the released medium. As shown in Fig. 5, the release of the Cs-E/B-ATT from its different formulae can be ranked in the following descending order; (E2 > E3 > E1) and (B2 > B3 > B1). It's clear that the drug release varied from (83.88–93.2%) and (87.7–97.35%) for Cs-EATT and



Cs-BATT, respectively. The maximum of Cs-E/B-ATT release was achieved from the HEC-based film (E2, B2). This phenomenon can be attributed to the molecular weight of both formulas (E2/B2) which is bigger than others, which leads to a higher release rate of the film dressing. An increase in polymer macromolecule cross-linking is stated to be a direct result of an increase in polymer molecular weight coupled by a decrease in polymer dissolution rate. As a result, the water and drug diffusion coefficients drop, and drug release decreases [47].

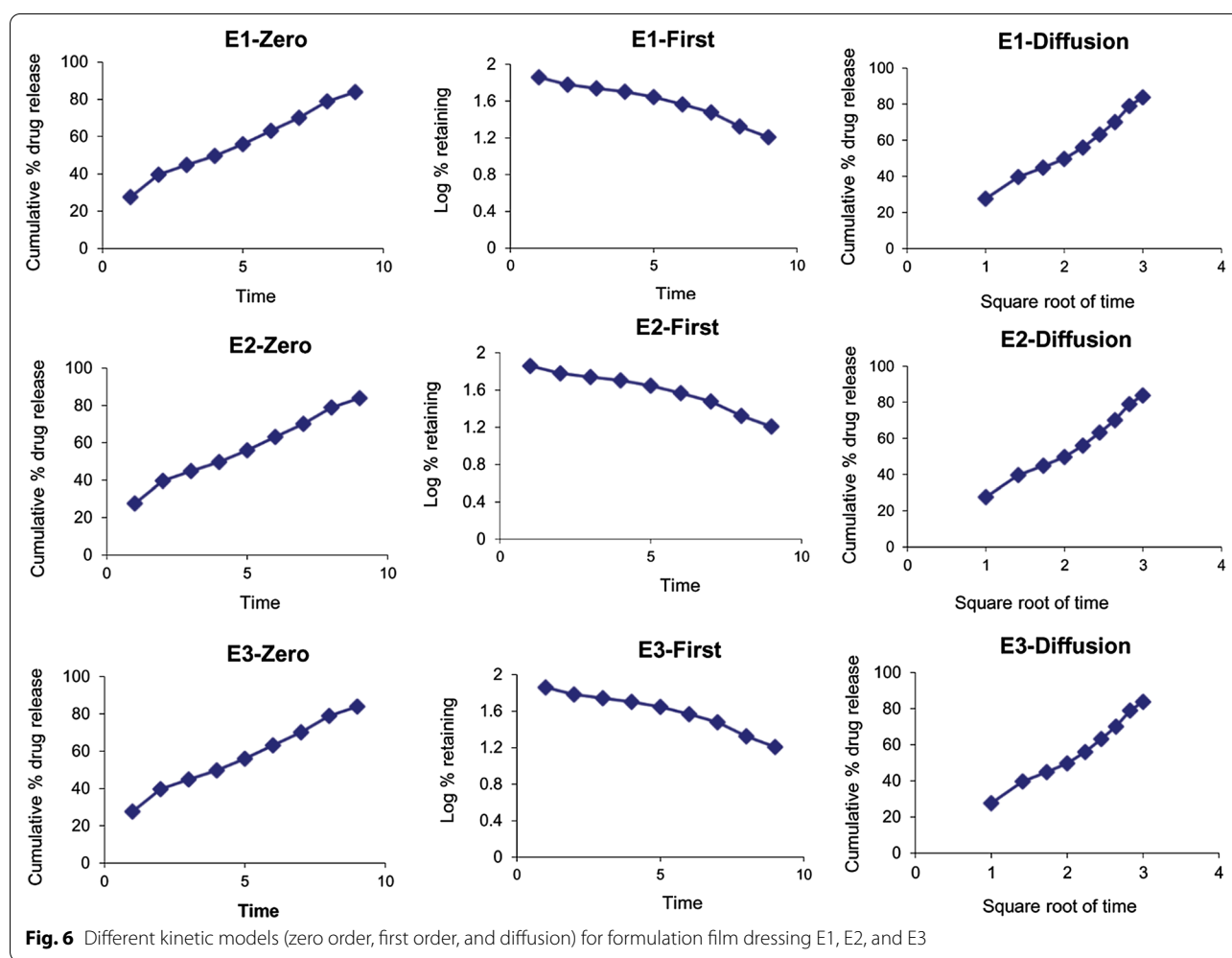
Kinetic analysis

The *in-vitro* release studies of Cs-E/ B-ATT as topical film dressings were represented in Table 7. Various kinetic models, including zero-order (cumulative % drug release vs. time), first-order (log cumulative % drug remaining vs. time), and diffusion models (Figs. 6 and 7) were applied to obtain the best fit for the results. Data showed that the *in-vitro* release of Cs-E/ B-ATT films followed zero transport. Therefore, the release of drugs from the formulated films is controlled by the swelling of the polymer, followed by drug diffusion through the polymer and slow erosion of the polymer, representing constant drug release in zero-order kinetics from the wound dressing films. The zero-order release model represents ideal drug delivery to maintain constant drug release as in transdermal patches and matrix tablets [75].

Table 7 Kinetics of the in-vitro release of Cs-E/B-ATT film dressing

Formula	Zero-order		First-order		Diffusion		$t_{1/2}$	Release Model
	R^2	K_0	R^2	K_1	R^2	k_H		
E1	0.996272	6.7855	-0.9753	-0.1783	0.988634	27.54107	7.368654	Zero
E2	0.997622	6.842167	-0.9696	-0.2616	0.994952	27.91073	7.307627	Zero
E3	0.999117	6.244167	-0.9734	-0.1927	0.991228	25.33804	8.007474	Zero
B1	0.986033	6.7665	-0.9776	-0.2172	0.976768	27.41608	7.389345	Zero
B2	0.99288	7.680833	-0.9334	-0.3578	0.978396	30.95761	6.50971	Zero
B3	0.990826	7.034167	-0.9728	-0.2679	0.982437	28.52732	7.108163	Zero

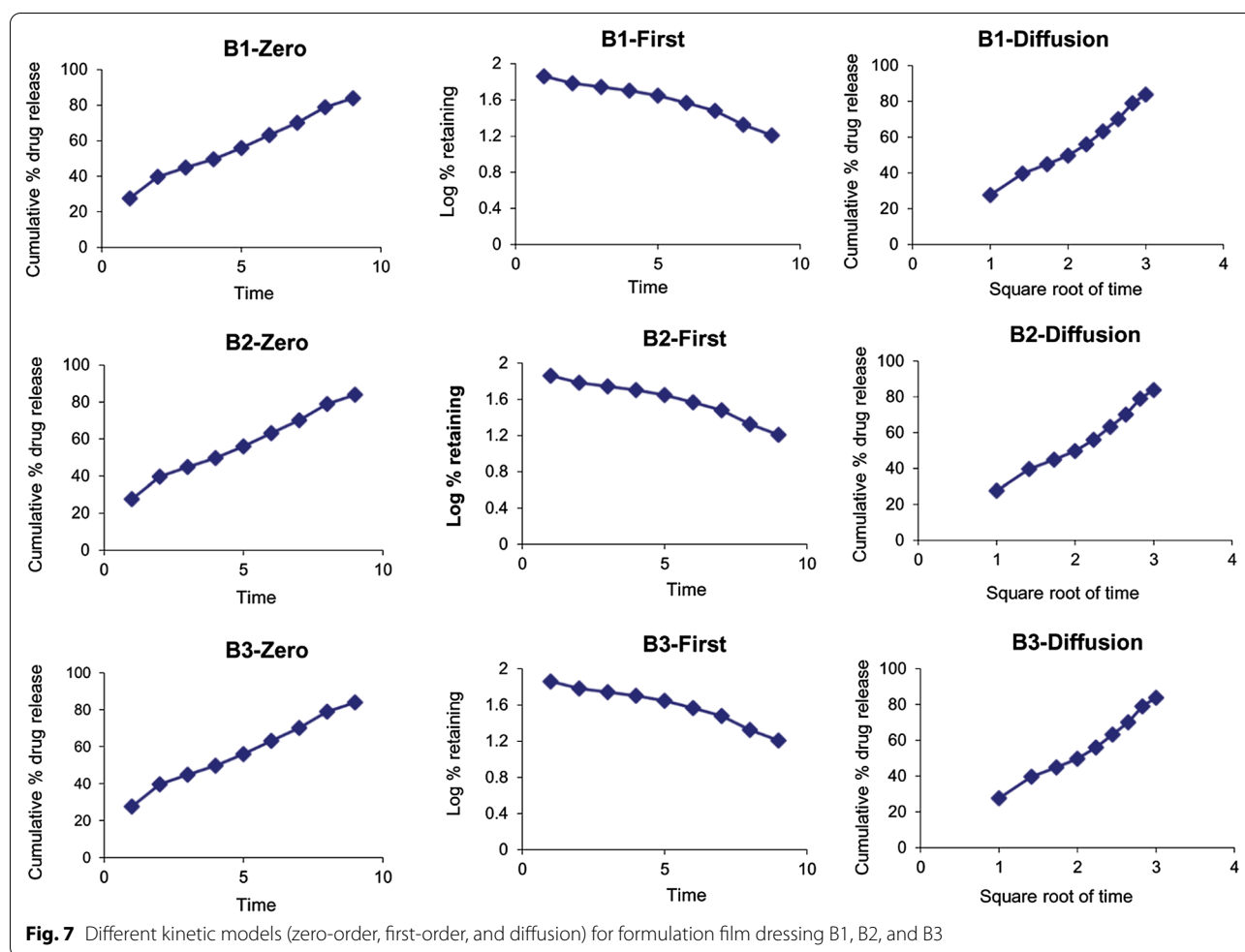
K_0 is the zero-order rate constant; K_1 is the first-order rate constant; K_H is the Higuchi constant



Conclusions

In this work, functionalization of chitosan with thiaziazole-based compounds was achieved to form two polymers, Cs-EATT and Cs-BATT, which were confirmed by FT-IR and ¹H-NMR. The DS was calculated from the elemental analysis and it was 84.7% and 44.1% for

Cs-EATT and Cs-BATT, respectively. The TGA result showed that the thermal stability of Cs-BATT is higher than that of Cs-EATT. The activities of Cs-EATT and Cs-BATT against the growth of *S. aureus*, *B. subtilis*, *E. coli*, *P. aeruginosa*, and *C. albicans* were assessed, and the results showed that the activity of Cs-EATT was



higher than that of Cs-BATT against all tested organisms except *C. albicans*. Also, data analysis revealed that the antimicrobial activity of two synthesized polymers was decreased by decreasing their concentration. The MIC values for Cs-EATT against *B. subtilis*, *S. aureus*, *P. aeruginosa*, *E. coli*, and *C. albicans* were 25, 25, 50, 50, and 100 $\mu\text{g mL}^{-1}$, respectively, whereas they were 100, 200, 100, 100, and 25 $\mu\text{g mL}^{-1}$ for Cs-BATT with varied clear zones. The dressing films were successfully fabricated by the solution methods using PVA, HEC, and CMC as film-forming agents. The physical characterization of the obtained films was assessed. The results indicated good transparency of PVA and HEC based films and that the maximum folding endurance and tensile strength were observed for PVA films. The pH values of the films were acceptable (6.1–6.9), avoiding the risk of skin irritation when they were applied. The highest Cs-E/B-ATT content was recorded for HEC formulations. The in-vitro release of Cs-E/B-ATT was investigated using the dialysis membrane as the release medium, and the results indicated the

maximum Cs-E/B-ATT release from the HEC-based film. The obtained data paved the way for the functionalization of chitosan with a variety of thiazazole-based compounds to produce biopolymers for various biomedical applications.

Supplementary Information

The online version contains supplementary material available at <https://doi.org/10.1186/s13765-022-00725-7>.

Additional file 1: Figure S1. Fourier-transform infrared spectra of (a) E-ATTA, (b) Cs, and (c) Cs-EATT. **Figure S2.** Fourier-transform infrared spectra of (a) B-ATTA, (b) Cs, and (c) Cs-BATT. **Figure S3.** (a) $^1\text{H-NMR}$ of E-ATTA, (b) $^1\text{H-NMR/D}_2\text{O}$ of E-ATTA, and (c) $^{13}\text{C-NMR}$ of E-ATTA. **Figure S4.** (a) $^1\text{H-NMR}$ and (b) $^{13}\text{C-NMR}$ of B-ATTA.

Acknowledgements

We are grateful for the consistent support of Al-Azhar University's faculty of science (boys) and faculty of pharmacy (girls) throughout this study.

Author contributions

AEM: methodology, software, formal analysis, data curation, resources, and writing—original draft. WEE: conceptualization, methodology, validation, formal analysis, data curation, writing—original draft, and writing—review

and editing. AMD: methodology, validation, formal analysis, data curation, and writing—original draft. AG: conceptualization, methodology, validation, formal analysis, data curation, supervision, writing—original draft, and writing—review and editing. AF: conceptualization, methodology, software, formal analysis, data curation, writing—original draft, and writing—review and editing. SMH: conceptualization, validation, resources, and supervision. All authors read and approved the final manuscript.

Funding

Open access funding provided by The Science, Technology & Innovation Funding Authority (STDF) in cooperation with The Egyptian Knowledge Bank (EKB).

Availability of data and materials

Request for the raw data used in this study will be fulfilled.

Declarations

Competing interests

The authors declare that they have no competing interests.

Author details

¹Department of Chemistry, Faculty of Science (Boys), Al-Azhar University, El-Nasr road, Nasr city, Cairo 11751, Egypt. ²Department of Pharmaceutics and Pharmaceutical Technology, Faculty of Pharmacy (Girls), Al-Azhar University, Cairo, Egypt. ³Department of Botany and Microbiology, Faculty of Science (Boys), Al-Azhar University, Cairo, Egypt.

Received: 27 May 2022 Accepted: 31 July 2022

Published online: 11 August 2022

References

- Liang N, Sun S, Li X, Piao H, Piao H, Cui F, Fang L (2012) α -Tocopherol succinate-modified chitosan as a micellar delivery system for paclitaxel: preparation, characterization and in vitro/in vivo evaluations. *Int J Pharm* 423:480–488
- Chen Y-C, Ho H-O, Lee T-Y, Sheu M-T (2013) Physical characterizations and sustained release profiling of gastroretentive drug delivery systems with improved floating and swelling capabilities. *Int J Pharm* 441:162–169
- Al-Zubiady SF, Al-Khafaji ZHK, Mohamed IM (2018) Synthesis, characterization of new 1, 3, 4-thiadiazole derivatives with studying their biological activity. *Res J Pharm Technol* 11:284–293
- Mojallal-Tabatabaei Z, Foroumadi P, Toolabi M, Goli F, Moghimi S, Kaboudanian-Ardestani S, Foroumadi A (2019) 2-(Bipiperidin-1-yl)-5-(nitroaryl)-1, 3, 4-thiadiazoles: synthesis, evaluation of in vitro leishmanicidal activity, and mechanism of action. *Bioorg Med Chem* 27:3682–3691
- Yan L, Deng M, Chen A, Li Y, Zhang W, Du Z-y, Dong C-z, Meunier B, Chen H (2019) Synthesis of N-pyrimidin [1, 3, 4] oxadiazoles and N-pyrimidin [1, 3, 4]-thiadiazoles from 1, 3, 4-oxadiazol-2-amines and 1, 3, 4-thiadiazol-2-amines via Pd-catalyzed heteroarylation. *Tetrahedron Lett* 60:1359–1362
- Muğlu H, Yakan H, Shouaib HA (2020) New 1, 3, 4-thiadiazoles based on thiophene-2-carboxylic acid: synthesis, characterization, and antimicrobial activities. *J Mol Struct* 1203:127470
- Muğlu H, Şener N, Emsaed HAM, Özkınalı S, Özkan OE, Gür M (2018) Synthesis and characterization of 1, 3, 4-thiadiazole compounds derived from 4-phenoxybutyric acid for antimicrobial activities. *J Mol Struct* 1174:151–159
- Jakovljević K, Matić IZ, Stanojković T, Krivokuća A, Marković V, Joksović MD, Mihailović N, Nićiforović M, Joksović L (2017) Synthesis, antioxidant and antiproliferative activities of 1, 3, 4-thiadiazoles derived from phenolic acids. *Bioorg Med Chem Lett* 27:3709–3715
- Zhang J, Wang X, Yang J, Guo L, Wang X, Song B, Dong W, Wang W (2020) Novel diosgenin derivatives containing 1, 3, 4-oxadiazole/thiadiazole moieties as potential antitumor agents: design, synthesis and cytotoxic evaluation. *Eur J Med Chem* 186:111897
- Quintana C, Klahn AH, Artigas V, Fuentealba M, Biot C, Halloum I, Kremer L, Arancibia R (2015) Cyrhetyrenyl and ferrocenyl 1, 3, 4-thiadiazole derivatives: synthesis, characterization, crystal structures and in vitro antitubercular activity. *Inorg Chem Commun* 55:48–50
- Haider S, Alam MS, Hamid H, Dhulap A, Kumar D (2019) Design, synthesis and biological evaluation of benzoxazolinone-containing 1, 3, 4-thiadiazoles as TNF- α inhibitors. *Heliyon* 5:e01503
- Luszczki JJ, Karpińska M, Matysiak J, Niewiadomy A (2015) Characterization and preliminary anticonvulsant assessment of some 1, 3, 4-thiadiazole derivatives. *Pharmacol Rep* 67:588–592
- Jakovljević K, Joksović MD, Botta B, Jovanović LS, Avdović E, Marković Z, Mihailović V, Andrić M, Trifunović S, Marković V (2019) Novel 1, 3, 4-thiadiazole conjugates derived from protocatechuic acid: synthesis, antioxidant activity, and computational and electrochemical studies. *C R Chimie* 22:585–598
- Sadat-Ebrahimi SE, Mirmohammadi M, Tabatabaei ZM, Arani MA, Jafari-Ashtiani S, Hashemian M, Foroumadi P, Yahya-Meymandi A, Moghimi S, Moshafi MH (2019) Novel 5-(nitrothiophene-2-yl)-1, 3, 4-thiadiazole derivatives: synthesis and antileishmanial activity against promastigote stage of leishmania major. *Iran J Pharm Res* 18:1816
- Chen J, Yi C, Wang S, Wu S, Li S, Hu D, Song B (2019) Novel amide derivatives containing 1, 3, 4-thiadiazole moiety: design, synthesis, nematocidal and antibacterial activities. *Bioorg Med Chem Lett* 29:1203–1210
- Er M, Özer A, Direkel Ş, Karakurt T, Tahtaci H (2019) Novel substituted benzothiazole and Imidazo [2, 1-b][1, 3, 4] thiadiazole derivatives: synthesis, characterization, molecular docking study, and investigation of their in vitro antileishmanial and antibacterial activities. *J Mol Struct* 1194:284–296
- Fascio ML, Sepúlveda CS, Damonte EB, D'Accorso NB (2019) Synthesis and antiviral activity of some imidazo [1, 2-b][1, 3, 4] thiadiazole carbohydrate derivatives. *Carbohydr Res* 480:61–66
- Chawla G, Kumar U, Bawa S, Kumar J (2012) Syntheses and evaluation of anti-inflammatory, analgesic and ulcerogenic activities of 1, 3, 4-oxadiazole and 1, 2, 4-triazolo [3, 4-b]-1, 3, 4-thiadiazole derivatives. *J Enzyme Inhib Med Chem* 27:658–665
- Kaur H, Kumar S, Vishwakarma P, Sharma M, Saxena KK, Kumar A (2010) Synthesis and antipsychotic and anticonvulsant activity of some new substituted oxa/thiadiazolylazetidinyloxy/thiazolidinonylcarbazoles. *Eur J Med Chem* 45:2777–2783
- Oruç EE, Rollas S, Kandemirli F, Shvets N, Dimoglo AS (2004) 1, 3, 4-thiadiazole derivatives. Synthesis, structure elucidation, and structure—antituberculosis activity relationship investigation. *J Med Chem* 47:6760–6767
- Yusuf M, Khan RA, Ahmed B (2008) Syntheses and anti-depressant activity of 5-amino-1, 3, 4-thiadiazole-2-thiol imines and thiobenzyl derivatives. *Bioorg Med Chem* 16:8029–8034
- Turner S, Myers M, Gadie B, Nelson AJ, Pape R, Saville JF, Doxey JC, Berridge TL (1988) Antihypertensive thiadiazoles. 1. Synthesis of some 2-aryl-5-hydrazino-1, 3, 4-thiadiazoles with vasodilator activity. *J Med Chem* 31:902–906
- Ibrahim AG, Saleh AS, Elsharma EM, Metwally E, Siyam T (2019) Chitosan-g-maleic acid for effective removal of copper and nickel ions from their solutions. *Int J Biol Macromol* 121:1287–1294
- El-Naggar MM, Haneen DSA, Mehany ABM, Khalil MT (2020) New synthetic chitosan hybrids bearing some heterocyclic moieties with potential activity as anticancer and apoptosis inducers. *Int J Biol Macromol* 150:1323–1330
- Gamal A, Ibrahim AG, Eliwa EM, El-Zomrawy AH, El-Bahy SM (2021) Synthesis and characterization of a novel benzothiazole functionalized chitosan and its use for effective adsorption of Cu(II). *Int J Biol Macromol* 183:1283–1292
- Möller H, Grelier S, Pardon P, Coma V (2004) Antimicrobial and physico-chemical properties of chitosan—HPMC-based films. *J Agric Food Chem* 52:6585–6591
- Sudatta BP, Sugumar V, Varma R, Nigariga P (2020) Extraction, characterization and antimicrobial activity of chitosan from pen shell, Pinna bicolor. *Int J Biol Macromol* 163:423–430
- Xing K, Li TJ, Liu YF, Zhang J, Zhang Y, Shen XQ, Li XY, Miao XM, Feng ZZ, Peng X (2018) Antifungal and eliciting properties of chitosan against *Ceratocystis fimbriata* in sweet potato. *Food Chem* 268:188–195
- Avelelas F, Horta A, Pinto LFV, Cotrim Marques S, Marques Nunes P, Pedrosa R, Leandro SM (2019) Antifungal and antioxidant properties

- of chitosan polymers obtained from nontraditional *Polybius henslowii* sources. *Mar Drugs* 17:239
30. Alharbi WS, Almughem FA, Almeahmady AM, Jarallah SJ, Alsharif WK, Alzaharani NM, Alshehri AA (2021) Phytosomes as an emerging nanotechnology platform for the topical delivery of bioactive phytochemicals. *Pharm* 13:1475
 31. Patel J, Patel B, Banwait H, Parmar K, Patel M (2011) Formulation and evaluation of topical aceclofenac gel using different gelling agent. *Int J Drug Dev Res* 3:156–164
 32. Sanjay D, Bhaskar M, Patel JR (2009) Enhanced percutaneous permeability of acyclovir by dmso from topical gel formulation. *Int J Pharm Sci Drug Res* 1(1):13–18
 33. Bayat M, Fox JM (2016) An efficient one-pot synthesis of bis butenolides. *J Heterocycl Chem* 53:1661–1664
 34. Montazer MN, Asadi M, Bahadorikhallil S, Hosseini FS, Amanlou A, Biglar M, Amanlou M (2021) Design, synthesis, docking study and urease inhibitory activity evaluation of novel 2-((5-amino-1, 3, 4-thiadiazol-2-yl) thio)-N-arylacetamide derivatives. *Med Chem Res* 30:729–742
 35. Mohamed AE, Elgammal WE, Eid AM, Dawaba AM, Ibrahim AG, Fouda A, Hassan SM (2022) Synthesis and characterization of new functionalized chitosan and its antimicrobial and in-vitro release behavior from topical gel. *Int J Biol Macromol* 207:242–253
 36. Aghcheli A, Toolabi M, Ayati A, Moghimi S, Firoozpour L, Bakhshaiesh TO, Nazeri E, Norouzbahari M, Esmaeili R, Foroumadi A (2020) Design, synthesis, and biological evaluation of 1-(5-(benzylthio)-1, 3, 4-thiadiazol-2-yl)-3-phenylurea derivatives as anticancer agents. *Med Chem Res* 29:2000–2010
 37. Ruan X, Zhang C, Jiang S, Guo T, Xia R, Chen Y, Tang X, Xue W (2018) Design, synthesis, and biological activity of novel myricetin derivatives containing amide, thioether, and 1, 3, 4-thiadiazole moieties. *Molecules* 23:3132
 38. Valgas C, Souza S, SmâniaSmânia EFAA Jr (2007) Screening methods to determine antibacterial activity of natural products. *Braz J Microbiol* 38:369–380
 39. Abd-Elaziz AM, Aly HM, Saleh NM, Fouad SA, Ismail AA, Fouda A (2021) Synthesis and characterization of the novel pyrimidine's derivatives, as a promising tool for antimicrobial agent and in-vitro cytotoxicity. *J Iran Chem Soc* 19(6):2279–2296
 40. Gonelimali FD, Lin J, Miao W, Xuan J, Charles F, Chen M, Hatab SR (2018) Antimicrobial properties and mechanism of action of some plant extracts against food pathogens and spoilage microorganisms. *Front Microbiol* 9:1639
 41. El-Belely EF, Farag MMS, Said HA, Amin AS, Azab E, Gobouri AA, Fouda A (2021) Green synthesis of zinc oxide nanoparticles (ZnO-NPs) using *arthrosira platensis* (Class: Cyanophyceae) and evaluation of their biomedical activities. *Nanomaterials* 11(1):95
 42. Kumar B, Jain SK, Prajapati SK (2011) Effect of penetration enhancer DMSO on in-vitro skin permeation of acyclovir transdermal microemulsion formulation. *Int J Drug Deliv* 3(1):83–94
 43. Suyatma NE, Tighzert L, Copinet A, Coma V (2005) Effects of hydrophilic plasticizers on mechanical, thermal, and surface properties of chitosan films. *J Agric Food Chem* 53:3950–3957
 44. Ahmed MG, Harish NM, Charyulu RN, Prabhu P (2009) Formulation of chitosan-based ciprofloxacin and diclofenac film for periodontitis therapy. *Trop J Pharm Res* 8:33–41
 45. Irfan M, Rabel S, Bukhtar Q, Qadir MI, Jabeen F, Khan A (2016) Orally disintegrating films: a modern expansion in drug delivery system. *Saudi Pharm J* 24:537–546
 46. Koteswari P, Sravanthi GP, Mounika M, Rafi SKM, Nirosha K (2016) Formulation development and evaluation of zolmitriptan oral soluble films using 22 factorial designs. *Int J Pharm Investig* 6:201
 47. Dawaba HM, Dawaba AM (2019) Development and evaluation of extended release ciprofloxacin HCl ocular inserts employing natural and synthetic film forming agents. *J Pharm Invest* 49:245–257
 48. Ashara KC, Paun JS, Soniwala MM, Chavada JR, Mori NM (2014) Microemulsion based emulgel: a novel topical drug delivery system. *Asian Pac J Trop Dis* 4:527–532
 49. Zade PS, Kawtikwar PS, Sakarkar DM (2009) Formulation, evaluation and optimization of fast dissolving tablet containing tizanidine hydrochloride. *Int J Pharm Tech Res* 1:34–42
 50. Sandulovici R, Prasacu I, Mircioiu C, Voicu V, Medvedovici A, Anuta V (2009) Mathematical and phenomenological criteria in selection of pharmacokinetic model for M1 metabolite of pentoxifylline. *Farmacologia* 57:235–247
 51. Siepmann J, Siepmann F (2011) Mathematical modeling of drug release from lipid dosage forms. *Int J Pharm* 418:42–53
 52. Mircioiu C, Voicu V, Anuta V, Tudose A, Celia C, Paolino D, Fresta M, Sandulovici R, Mircioiu I (2019) Mathematical modeling of release kinetics from supramolecular drug delivery systems. *Pharm* 11:140
 53. Wang Y, Dang Q, Liu C, Yu D, Pu X, Wang Q, Gao H, Zhang B, Cha D (2018) Selective adsorption toward Hg (II) and inhibitory effect on bacterial growth occurring on thiosemicarbazide-functionalized chitosan microsphere surface. *ACS Appl Mater Interfaces* 10:40302–40316
 54. Zhang H, Dang Q, Liu C, Cha D, Yu Z, Zhu W, Fan B (2017) Uptake of Pb (II) and Cd (II) on chitosan microsphere surface successively grafted by methyl acrylate and diethylenetriamine. *ACS Appl Mater Interfaces* 9:11144–11155
 55. Baran T, Menteş A (2015) Cu(II) and Pd(II) complexes of water soluble O-carboxymethyl chitosan Schiff bases: synthesis, characterization. *Int J Biol Macromol* 79:542–554
 56. Li Q, Zhang C, Tan W, Gu G, Guo Z (2017) Novel amino-pyridine functionalized chitosan quaternary ammonium derivatives: design, synthesis, and antioxidant activity. *Molecules* 22(1):156
 57. Hamza MF, Hamad DM, Hamad NA, Abdel-Rahman AAH, Fouda A, Wei Y, Guibal E, El-Etrawy A-AS (2022) Functionalization of magnetic chitosan microparticles for high-performance removal of chromate from aqueous solutions and tannery effluent. *Chem Eng J* 428:131775
 58. Cheung RC, Ng TB, Wong JH, Chan WY (2015) Chitosan: an update on potential biomedical and pharmaceutical applications. *Mar Drugs* 13:5156–5186
 59. Li Q, Ren J, Dong F, Feng Y, Gu G, Guo Z (2013) Synthesis and antifungal activity of thiadiazole-functionalized chitosan derivatives. *Carbohydr Res* 373:103–107
 60. Mujeeb Rahman P, Muraleedaran K, Mujeeb VM (2015) Applications of chitosan powder with in situ synthesized nano ZnO particles as an antimicrobial agent. *Int J Biol Macromol* 77:266–272
 61. Hamza MF, Fouda A, Elwakeel KZ, Wei Y, Guibal E, Hamad NA (2021) Phosphorylation of guar gum/magnetite/chitosan nanocomposites for uranium (VI) sorption and antibacterial applications. *Molecules* 26(7):1920
 62. Kumar D, Gihar S, Shrivash MK, Kumar P, Kundu PP (2020) A review on the synthesis of graft copolymers of chitosan and their potential applications. *Int J Biol Macromol* 163:2097–2112
 63. Sudarshan NR, Hoover DG, Knorr D (1992) Antibacterial action of chitosan. *Food Biotechnol* 6:257–272
 64. Zheng L-Y, Zhu J-F (2003) Study on antimicrobial activity of chitosan with different molecular weights. *Carbohydr Polym* 54:527–530
 65. Patale RL, Patravale VB (2011) O, N-carboxymethyl chitosan–zinc complex: a novel chitosan complex with enhanced antimicrobial activity. *Carbohydr Polym* 85(1):105–110
 66. Fouda A, Hassan SE-D, Saied E, Hamza MF (2021) Photocatalytic degradation of real textile and tannery effluent using biosynthesized magnesium oxide nanoparticles (MgO-NPs), heavy metal adsorption, phytotoxicity, and antimicrobial activity. *J Environ Chem Eng* 9:105346
 67. Hamza MF, Fouda A, Wei Y, El Aassy IE, Alotaibi SH, Guibal E, Mashaal NM (2021) Functionalized biobased composite for metal decontamination—insight on uranium and application to water samples collected from wells in mining areas (Sinai, Egypt). *Chem Eng J* 431:133967
 68. Veeraswamy B, Madhu D, Jitender Dev G, Poornachandra Y, Shrvan Kumar G, Ganesh Kumar C, Narsaiah B (2018) Studies on synthesis of novel pyrido[2,3-d]pyrimidine derivatives, evaluation of their antimicrobial activity and molecular docking. *Bioorg Med Chem Lett* 28:1670–1675
 69. Salahuddin N, Elbarbary A, Allam NG, Hashim AF (2018) Chitosan modified with 1, 3, 4-oxa (thia) diazole derivatives with high efficacy to heal burn infection by *Staphylococcus aureus*. *J Bioact Compat Polym* 33:254–268
 70. Kenawy E-R, Elbarbary AA, Hamada EGI (2019) Modification of chitosan and polymethyl methacrylate with 5-phenyl-1, 3, 4-oxadiazole derivatives and their antifungal activity. *Delta J Sci* 40:59–70

71. Ahmad M, Ahmed S, Swami BL, Ikram S (2015) Preparation and characterization of antibacterial thiosemicarbazide chitosan as efficient Cu (II) adsorbent. *Carbohydr polym* 132:164–172
72. Nithiyananthan TS, Shankarananth V, Rajasekhar KK, Jyothikrishna K, Mukesh O, Vikram KE (2009) Preparation and evaluation of ciprofloxacin ocuserts. *J Pharm Res* 2:1496–1499
73. Asrofi M, Dwilaksana D, Abral H, Fajrul R (2019) Tensile, thermal and moisture absorption properties of polyvinyl alcohol (PVA)/bengkuang (*Pachyrhizus erosus*) starch blend films. *Mater Sci Res India* 16:70–75
74. Asrofi M, Abral H, Putra YK, Sapuan SM, Kim HJ (2018) Effect of duration of sonication during gelatinization on properties of tapioca starch water hyacinth fiber biocomposite. *Int J Biol Macromol* 108:167–176
75. Singhvi G, Singh M (2011) In-vitro drug release characterization models. *Int J Pharm Stud Res* 2:77–84

Publisher's Note

Springer Nature remains neutral with regard to jurisdictional claims in published maps and institutional affiliations.

Submit your manuscript to a SpringerOpen[®] journal and benefit from:

- ▶ Convenient online submission
- ▶ Rigorous peer review
- ▶ Open access: articles freely available online
- ▶ High visibility within the field
- ▶ Retaining the copyright to your article

Submit your next manuscript at ▶ [springeropen.com](https://www.springeropen.com)
